

Optical injection and coherent control of a ballistic charge current in GaAs/AlGaAs quantum wells

Martin J. Stevens

Laboratory for Photonics and Quantum Electronics, 138 IATL, University of Iowa, Iowa City, Iowa 52242

Ali Najmaie, R. D. R. Bhat, J. E. Sipe, and H. M. van Driel

Department of Physics, University of Toronto, 60 St. George Street, Toronto, Ontario M5S 1A7, Canada

Arthur L. Smirl^{a)}

Laboratory for Photonics and Quantum Electronics 138 IATL, University of Iowa, Iowa City, Iowa 52242

(Received 2 July 2003; accepted 23 July 2003)

We report all-optical injection and coherent control of a ballistic charge current in GaAs/AlGaAs quantum wells. This current arises through quantum interference of one- and two-photon absorption of ~ 100 fs pulses with parallel linear polarizations, and its magnitude can be controlled by adjusting the relative phase of the incident pulses. By monitoring differential transmission using a spatially resolved optical pump-probe technique, we observe evidence of carrier motion associated with this ballistic current. Results are consistent with a theoretical treatment specific to quantum wells, and are qualitatively similar to previous measurements in bulk GaAs. © 2003 American Institute of Physics. [DOI: 10.1063/1.1609639]

I. INTRODUCTION

Charge currents in semiconductors form the backbone of modern solid state electronics, where charge carriers are typically manipulated by an applied external bias. Recently, however, a number of experiments have shown that it is possible to directly inject ballistic currents optically into unbiased semiconductors through quantum interference of multiple excitation pathways connecting initial and final states.¹⁻⁹ In one scheme, quantum interference and control (QUIC)⁴ of two- and one-photon absorption processes induced by fundamental (ω) and second harmonic (2ω) pulses with parallel linear polarizations was used to produce carriers distributed asymmetrically in k space, thus generating a net charge current.²⁻⁴ Haché *et al.*^{2,3} studied this current in bulk GaAs by monitoring charge collection using conventional electrodes, and they demonstrated very large current densities of ~ 1 kA/cm² with carrier densities of only $\sim 10^{14}$ cm⁻³, owing to the very high average velocities (>500 km/s) of electrons associated with these ballistic currents.³ In addition, the carrier motion associated with this QUIC current has been used to generate THz emission.¹⁰ In contrast to recent predictions^{11,12} and demonstrations⁷⁻⁹ of QUIC spin currents for other incident polarizations, this current is not expected to be spin polarized.^{11,12}

Here, we report generation of a ballistic charge current for parallel linear ω and 2ω polarizations, similar to the work of Haché *et al.*,^{2,3} but in this article we report injection into the plane of GaAs/AlGaAs quantum wells instead of bulk GaAs. Furthermore, rather than using electrodes to monitor this current, we use a spatially resolved optical pump-probe technique to study the resulting carrier motion. We demon-

strate that the magnitude and direction of this current can be coherently controlled by adjusting the relative phases of the optical pulses, qualitatively consistent both with previous results in bulk and with calculations specific to quantum wells.

Although we expect the underlying physics of injection and control of currents due to interference between one- and two-photon absorption processes to be the same in a quantum well as it is in bulk, confinement along the growth axis of the quantum well leads to energy states that are clearly different than in bulk. In addition, the barriers in a quantum well structure can restrict the carrier motion along the growth axis and alter the scattering processes of carriers traveling in the plane of the well. Thus, optically injecting, controlling and probing ballistic charge currents in the plane of a quantum well allows the possibility of studying ballistic transport in two dimensions without the use of an electrical bias.

II. QUANTUM INTERFERENCE CONTROL

For ω and 2ω with parallel linear polarizations and 2ω photon energy greater than the band gap, previous observations²⁻⁴ in *bulk* GaAs showed that QUIC leads to a net charge current along the direction of the incident optical polarizations. In this configuration, the optical polarization determines the direction of current flow. This previous work also showed that the magnitude and sign of this current could be coherently controlled by adjusting the relative phase of ω and 2ω fields that have parallel linear polarizations, through a relationship for current density injection rate, \mathbf{J} , of the form²⁻⁴

$$\mathbf{J} \propto |E(\omega)|^2 |E(2\omega)| \sin(\Delta\phi) \hat{\mathbf{r}}, \quad (1)$$

where $\Delta\phi \equiv 2\phi_\omega - \phi_{2\omega}$, ϕ_ω ($\phi_{2\omega}$) is the phase of the ω (2ω) field, $|E(\omega)|$ and $|E(2\omega)|$ are the field amplitudes, and

^{a)} Author to whom correspondence should be addressed; electronic mail: art-smirl@uiowa.edu

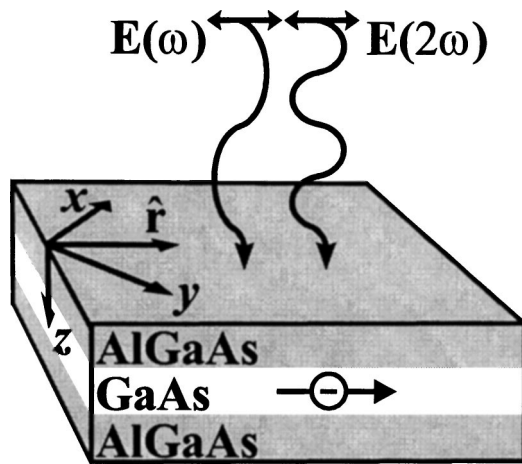


FIG. 1. Geometry for producing the ballistic charge current, with both ω and 2ω fields polarized along the \hat{f} direction, showing the ballistic motion of electrons in the $+\hat{f}$ direction.

\hat{f} is the polarization direction. In the present article, we will show that $\dot{\mathbf{J}}$ has the same qualitative behavior in quantum wells.

Figure 1 shows the situation we consider, where the ω and 2ω fields have parallel linear polarizations along the \hat{f} direction, and they are incident on a GaAs/AlGaAs quantum well structure. If the results in quantum wells are qualitatively similar to those in bulk, we expect to see a ballistic charge current injected along the \hat{f} direction, which will be in the plane of the quantum wells (the x - y plane), as Fig. 1 shows.

Note that this geometry is distinct from the report¹ of directional ionization of electrons from a *doped* quantum well structure through the interference of one- and two-photon absorption associated with *intraband* transitions, generating a current perpendicular to the plane of the wells.¹ By contrast, in the present work we inject currents *in the plane* of *undoped* quantum wells through *interband* transitions.

Figure 2(a) plots electron density as a function of position, showing the expected motion of the optically injected Gaussian electron distribution resulting from this ballistic

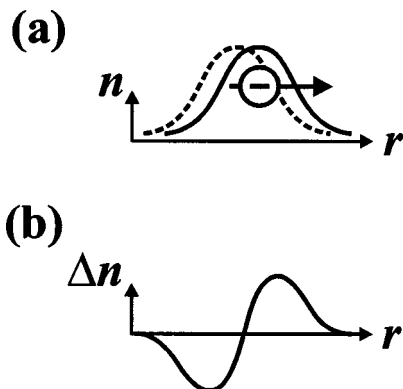


FIG. 2. (a) Schematic of the expected movement of the electron density spatial profile, n , from the initial position (dashed line) to the resultant position (solid line). (b) Change in electron density, Δn , resulting from this motion.

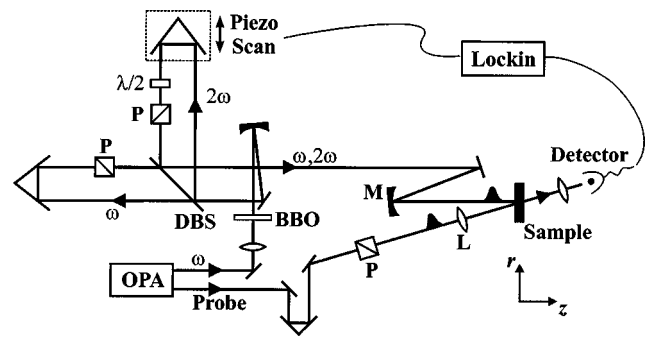


FIG. 3. Experimental geometry for measuring $\Delta T(n)$ and $\Delta T(\Delta\phi)$: DBS, P , and $\lambda/2$ represent a dichroic beamsplitter, a polarizer, and a half wave plate, respectively; L and M are a lens and a spherical curved mirror with focal lengths of 2 and 5 cm, respectively.

current, from its original position (dashed line), to the resultant position (solid line). For the case shown, the electron distribution moves in the $+\hat{f}$ direction. As Fig. 2(b) illustrates, this movement will result in a change in electron density as a function of position, $\Delta n(r)$, that approximates the spatial derivative of the original Gaussian profile, $\partial n/\partial r$, provided the movement is small. The distance the profile moves is determined in part by the number of carriers involved in the current, their ballistic velocities, and the momentum relaxation time. The motion in Fig. 2(a) is greatly exaggerated; for the carrier density ($\sim 1.6 \times 10^{17} \text{ cm}^{-3}$), lattice temperature (80 K) and excess energy ($\sim 200 \text{ meV}$) used in our experiments, we expect electron motion on the order of a few nm.

III. EXPERIMENTAL GENERATION AND DETECTION OF QUIC CHARGE CURRENT

To inject and detect this ballistic charge current, we use the spatially resolved pump-probe technique outlined in Fig. 3. The $\sim 110 \text{ fs}$ fundamental (ω) pulse, with wavelength centered at $1.42 \mu\text{m}$, is produced by an optical parametric amplifier (OPA) that is pumped by a Ti:sapphire laser-seeded regenerative amplifier with a repetition rate of 250 kHz. Second harmonic generation in beta barium borate (BBO) produces the 2ω pulse at $0.71 \mu\text{m}$. The ω and 2ω pulses are separated using a dichroic beamsplitter, and the relative phase between them is controlled with a scanning Michelson interferometer. The two pulses, which have parallel linear polarizations, are recombined collinearly, overlapped in time, and focused onto a multiple quantum well (MQW) sample at normal incidence.

The MQW sample has ten periods of 14-nm-wide GaAs wells alternating with 17-nm-thick $\text{Al}_{0.3}\text{Ga}_{0.7}\text{As}$ barriers grown on a (001)-oriented GaAs substrate. The sample is undoped, and no external bias is applied. The sample is mounted on a glass flat, and the GaAs substrate has been removed by selective etching to permit transmission measurements. As we will discuss in Sec. V, normal incidence excitation in (001)-oriented GaAs/AlGaAs quantum wells prevents quantum interference control of the *total* carrier density, which has been observed for other incidence angles.^{13,14}

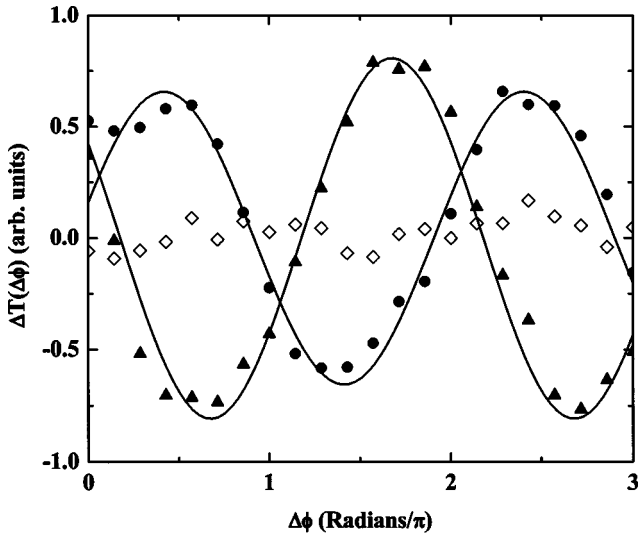


FIG. 4. Phase-dependent differential transmission [$\Delta T(\Delta\phi)$] vs relative phase parameter $\Delta\phi$, taken at $r \approx -7.5 \mu\text{m}$ (solid triangles), $r \approx 0$ (open diamonds), and $r \approx +7.5 \mu\text{m}$ (solid circles). Solid lines are sinusoidal fits to the data.

To monitor carrier movement resulting from the current, we use a tightly focused probe pulse that can be scanned along the \hat{r} direction across the region excited by the pumps. This linearly polarized probe, with wavelength $0.81 \mu\text{m}$, is derived from the remaining output of the regenerative amplifier after it has been used to pump the OPA.

The ω and 2ω pulses are focused to spot widths (full width half maximum) of $\sim 13 \mu\text{m}$ and $\sim 10 \mu\text{m}$, respectively, and the probe to $\sim 6 \mu\text{m}$. The peak irradiances are $\sim 5 \text{ GW/cm}^2$ for the ω pulse and $\sim 30 \text{ MW/cm}^2$ for the 2ω pulse. Acting independently, the ω and 2ω pulses each create peak carrier densities (at $r=0$) of $\sim 8 \times 10^{16} \text{ cm}^{-3}$ through two- and one-photon absorption, respectively. For all measurements, the sample is held at a temperature of 80 K, where the pumps generate electrons in the wells with excess energies of nearly 200 meV, which are low enough to keep electrons from being ionized out of the wells. In addition, the pumps do not create carriers in the barriers. The probe pulse is resonant with the heavy-hole exciton transition and arrives $\sim 4 \text{ ps}$ after the pumps to allow the ballistically injected hot carriers to thermalize.

IV. EXPERIMENTAL RESULTS

Figure 4 shows a measurement of the phase-dependent change in carrier density, $\Delta n(r, \Delta\phi)$: the phase-dependent change in probe transmission $\Delta T(\Delta\phi)$ is plotted as a function of the relative phase parameter, $\Delta\phi \equiv 2\phi_\omega - \phi_{2\omega}$, for three different probe positions. The center of the ω and 2ω spots is at $r=0$. To measure $\Delta T(\Delta\phi)$, a piezoelectric transducer attached to the retroreflector in the 2ω arm of the interferometer is periodically scanned to vary the relative phase of ω and 2ω pulses ($\Delta\phi$), and the piezo scanning frequency is used as the reference to a lock-in amplifier. For small changes in transmission, $\Delta T(\Delta\phi)$ is proportional to the change in carrier density at a given r position, $\Delta n(r, \Delta\phi)$.

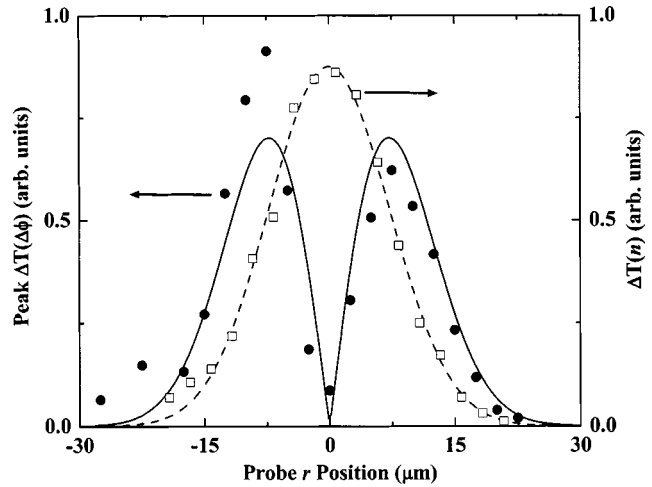


FIG. 5. Differential transmission vs probe r position. The open squares show $\Delta T(n)$, while the solid circles show the peak value of $\Delta T(\Delta\phi)$. The dashed line is a Gaussian fit to $\Delta T(n)$, and the solid line is the absolute value of the derivative of that Gaussian fit, scaled for comparison with the $\Delta T(\Delta\phi)$ data.

Consequently, Fig. 4 illustrates the phase dependence of $\Delta n(r, \Delta\phi)$ at three different probe positions. On the left side of the excitation region ($r \approx -7.5 \mu\text{m}$), Δn varies sinusoidally with $\Delta\phi$, and is approximately out of phase with Δn on the right side ($r \approx +7.5 \mu\text{m}$).¹⁵ For $\Delta\phi \approx \pi/2$, the carrier density increases on the right side of the excitation region while decreasing on the left side, showing a net motion of carriers to the right (in the $+\hat{r}$ direction). When $\Delta\phi$ changes by $\sim \pi$ (to $\sim 3\pi/2$), carriers move to the left (in the $-\hat{r}$ direction). We expect Δn at $r \approx -7.5 \mu\text{m}$ to be π out of phase with Δn at $r \approx +7.5 \mu\text{m}$; the deviation from π in the data is reproducible and occurs because the relative phase fronts of the ω and 2ω beams are not perfectly parallel. Most importantly, there is almost no phase dependence to Δn at $r \approx 0$, suggesting that an equal number of electrons move into and out of the probed region at $r \approx 0$ for any fixed $\Delta\phi$.

The solid circles in Fig. 5 show peak values of phase-dependent oscillations like those in Fig. 4, plotted for a range of probe positions. These solid circles are a measure of the maximum phase-dependent change in carrier density at each probe r position. For comparison, the open squares show the spatial profile of the background nonphase-dependent carrier density, $n(r)$. This overall density [$n(r)$] is monitored by inserting choppers in the pump and probe paths and using standard synchronous detection techniques to measure the change in probe transmission $\Delta T(n)$ with and without the pump pulses present.

Notice that the peak value of $\Delta T(\Delta\phi)$ as a function of r has approximately the same shape as $|\partial[\Delta T(n)]/\partial r|$ —hence the peak Δn has approximately the same shape as $|\partial n/\partial r|$ —verifying that there is carrier motion associated with a QUIC current. Controlling the relative phase parameter $\Delta\phi$ allows us to control whether this current travels in the $+\hat{r}$ or $-\hat{r}$ direction, as Fig. 4 illustrates.

By contrast, if there were a QUIC population change,^{13,14} Δn would have the same Gaussian spatial profile as n , Δn would be largest in the center, and the signals on the

left and right sides would be in phase. In addition, $\Delta T(\Delta\phi)$ is not a measure of diffusion, because transport arising from diffusion—while present—will be independent of phase.

Therefore, the data in Figs. 4 and 5 display the two most important features of the current previously observed in bulk GaAs and predicted by Eq. (1): (i) there is a net charge current injected along the direction of the ω and 2ω polarizations, and (ii) the magnitude and sign of this current can be coherently controlled by adjusting the relative phases of the ω and 2ω pulses.

The current reported here is distinct from recent reports of currents optically injected in unbiased semiconductors through the circular polarization galvanic effect¹⁶ and spin-galvanic effect.¹⁷ Among other reasons, our technique is only sensitive to a current that depends on the relative phase of ω and 2ω .

In addition, the ballistic *net charge current* reported here is very different from the ballistic *pure spin current* that was recently demonstrated,^{8,9} because in the case of the pure spin current, spin-up and spin-down currents had equal magnitude but traveled in opposite directions, yielding *no* net charge current.

V. THEORY OF QUIC CHARGE CURRENTS IN QUANTUM WELLS

In this section, we discuss a theoretical treatment of QUIC charge currents specific to quantum wells. A (001)-oriented zincblende quantum well, such as GaAs/AlGaAs, is invariant under the D_{2d} point group. We show that despite the different structure and symmetry of the quantum wells, the theoretical predictions are similar to those previously reported for bulk semiconductors, which are invariant under the T_d point group. Specifically, we calculate carrier density injection rates and current density injection rates; because the calculations are done for a quantum well, the densities discussed here are *areal* densities.

The theoretical description of coherent control of currents in semiconductors has been reviewed by van Driel and Sipe.⁴ Here we follow the theoretical framework outlined by Najmaie *et al.*¹² to study interference of quantum mechanical processes that lead to coherent control of ballistic currents in semiconductor quantum wells, and we refer to the literature for details of the geometries and the general theoretical description.^{4,12}

A. Coherent control

The quantum well we consider is excited by two monochromatic optical fields, of frequencies ω and 2ω , described by the electric field

$$\mathbf{E}(t) = \mathbf{E}(\omega)e^{-i\omega t} + \mathbf{E}(2\omega)e^{-i2\omega t} + \text{c.c.},$$

where c.c. denotes complex conjugate. We can use Fermi's golden rule to evaluate the expectation value of any *single* particle operator $\hat{\theta}$ and the time derivative of that operator $\dot{\theta} = d\langle\hat{\theta}\rangle/dt$ ¹²

$$\dot{\theta} = \dot{\theta}_1 + \dot{\theta}_2 + \dot{\theta}_I, \quad (2)$$

where $\dot{\theta}_1$ ($\dot{\theta}_2$) describes the time evolution of the operator $\hat{\theta}$ due to one (two) photon processes, and $\dot{\theta}_I$ is due to the interference between the quantum mechanical transition amplitudes at frequencies ω and 2ω . For any single particle operator $\hat{\theta}$, the time derivative $\dot{\theta}$ in Eq. (2) will include contributions from the conduction electrons and valence holes.

B. Carrier population

Following the general form of Eq. (2), the carrier density injection rate, $\dot{n} = d\langle\hat{n}\rangle/dt$, into the quantum well can be written

$$\dot{n} = \dot{n}_1 + \dot{n}_2 + \dot{n}_I,$$

where the one- and two-photon contributions to the carrier density injection rate are given by¹²

$$\dot{n}_1 = \xi_1^{ab} E^{a*}(2\omega) E^b(2\omega), \quad (3)$$

$$\dot{n}_2 = \xi_2^{abcd} E^{a*}(\omega) E^{b*}(\omega) E^c(\omega) E^d(\omega). \quad (4)$$

We sum over all repeated indices in expressions involving tensors in this article. From the time reversal properties of the matrix elements, it can be shown that in the independent particle picture ξ_1^{ab} and ξ_2^{abcd} are purely real.¹² Furthermore, reality of \dot{n}_1 and \dot{n}_2 leads to the constraints $\xi_1^{ab} = \xi_1^{ba}$ and $\xi_2^{abcd} = \xi_2^{cdab}$. We can also symmetrize ξ_2^{abcd} with respect to interchanging a and b , and with respect to interchanging c and d , since we sum over the repeated indices.

In general, if inversion asymmetry of the quantum well is neglected, then there is no contribution to the net carrier injection rates due to interference of transition amplitudes associated with one- and two-photon absorption, i.e., $\dot{n}_I = 0$.^{12,13} Moreover, even with a model that includes crystal asymmetry, for the experimental configuration considered in this article, where ω and 2ω fields propagate along the [001] direction, the point group symmetry of the quantum wells requires $\dot{n}_I = 0$. In both bulk GaAs (point group T_d) and GaAs/AlGaAs quantum wells (point group D_{2d}), \dot{n}_I is only nonzero when there is a projection of the ω field along at least two of the principle axes and the 2ω field has a projection along the third principle axis; for propagation in the [001] direction, neither ω nor 2ω has a field component along the [001] direction.^{13,14}

C. Charge currents

To calculate the charge current density injected in the quantum well, we use the charge current operator \hat{J}^a . Following Eq. (2), the charge current injection rate can be written

$$\dot{J}^a = \dot{J}_1^a + \dot{J}_2^a + \dot{J}_I^a.$$

The one- and two-photon current density injection rates, \dot{J}_1^a and \dot{J}_2^a , vanish for models that ignore the inversion asymmetry of the underlying crystal.^{12,18} In addition, the symmetries of the underlying crystal and experimental geometry consid-

ered here render these terms identically zero. The areal current density injected in the plane of the quantum well is due to the quantum mechanical interference between the one- and two-photon absorption processes, which takes the form

$$\hat{j}_I^a = \eta_I^{abcd} E^{b*}(\omega) E^{c*}(\omega) E^d(2\omega) + \text{c.c.} \quad (5)$$

The fourth rank tensor η_I^{abcd} can be symmetrized under the exchange of b and c , since the Cartesian indices in Eq. (5) are summed over. From time reversal properties of the matrix elements it follows that η_I^{abcd} is purely imaginary in the independent particle picture.¹²

The point group symmetry of the structure (D_{2d}) can be used to deduce the number of independent and nonzero elements of all the tensors discussed above. The fourth rank tensor η_I^{abcd} that describes charge current in Eq. (5) has 21 nonzero and eight independent tensor components.¹² The second rank tensor ξ_1^{ab} , which describes carrier population injection rate due to one photon absorption in Eq. (3), has three nonzero and two independent tensor components. The fourth rank tensor ξ_2^{abcd} used to describe carrier population injection *via* two photon absorption in Eq. (4) has 21 nonzero and six independent tensor components.

D. Parallel linear polarizations

To model our specific experimental configuration, we consider a single quantum well grown in the [001] direction, which we take as the z axis, as shown in Fig. 1. Although the experiments were performed in a MQW structure, the barriers are wide enough that we treat each well as an independent single quantum well. In the configuration where the ω and 2ω fields have parallel linear polarizations along the [110] direction,

$$\mathbf{E}(\omega/2\omega) = |E(\omega/2\omega)| e^{i\phi_{\omega/2\omega}} \frac{(\hat{\mathbf{x}} + \hat{\mathbf{y}})}{\sqrt{2}},$$

and are incident on the quantum well, the one- and two-photon carrier population injection rates are given by $\hat{n}_1 = \xi_1^{xx} |E(2\omega)|^2$ and $\hat{n}_2 = \frac{1}{2}(\xi_2^{xxxx} + \xi_2^{xyyy} + 2\xi_2^{xyxy}) |E(\omega)|^4$. In addition, a net ballistic charge current is injected in the plane of the quantum well along the direction of the field polarizations

$$\begin{aligned} \mathbf{J} = & \text{Im}(\eta_I^{xxxx} + \eta_I^{yyyy} \\ & + 2\eta_I^{xyxy}) |E(\omega)|^2 |E(2\omega)| \sin(\Delta\phi) \frac{(\hat{\mathbf{x}} + \hat{\mathbf{y}})}{\sqrt{2}}, \end{aligned} \quad (6)$$

as shown in Fig. 1. Clearly this equation has the same form as in bulk, as given by Eq. (1), and the magnitude and sign of this charge current can be controlled using the relative phase of the optical fields through the parameter $\Delta\phi \equiv 2\phi_\omega - \phi_{2\omega}$, which is in agreement with the data in Figs. 4 and 5. In addition, this current should consist of an equal number of “spin-up” and “spin-down” carriers, and thus it should not be spin polarized. In the experiments, the probe is linearly polarized; therefore our measurements do not differentiate between spin-up and spin-down carriers and are equally sensitive to both.

We can characterize the velocity with which the carriers are injected *via* the swarm velocity $\mathbf{v}_{\text{swarm}} = \mathbf{J}/(e\hat{n})$.⁴ The swarm velocity that characterizes the injected current in the present configuration is given by $v_{\text{swarm}}^a = (D\sqrt{\Xi})/(B + C\Xi)$, for $B = e\xi_1^{xx}$, $C = (e/4)(\xi_2^{xxxx} + \xi_2^{xyyy} + 2\xi_2^{xyxy})\sqrt{\mu_0/\epsilon_0}$, $D = \frac{1}{2}\text{Im}(\eta_I^{xxxx} + \eta_I^{xyyx} + 2\eta_I^{xyxy})(\mu_0/\epsilon_0)^{1/4}$, and the relative intensity parameter $\Xi = I_{2\omega}^2/I_{\omega}^2$, where the intensities of the beams are referred to by $I_{\omega/2\omega} = 2\sqrt{\epsilon_0/\mu_0}|E(\omega/2\omega)|^2$. The swarm velocity is maximized at $v_{\text{swarm}}^{\text{max}} = D/(2\sqrt{BC})$, for the relative intensity parameter $\Xi = B/C$. This corresponds to the situation where the one- and two-photon absorption rates are equal, i.e., $\hat{n}_1 = \hat{n}_2$; in the experiments, the condition $n_1 \approx n_2$ is satisfied.

The swarm velocity of injected electrons in a quantum well can be calculated using a model presented by Najmaie *et al.*,¹² where a 14 nm GaAs quantum well is described by a 4×4 isotropic Luttinger–Kohn model. For simplicity, the barriers are assumed to be infinite; since we only investigate the motion of the carriers in the plane of the well, this approximation does not alter any of the underlying physics. This theoretical treatment predicts that electrons can be injected with a swarm velocity of ~ 400 km/s for a 2ω photon energy of ~ 200 meV above the band gap and a relative intensity parameter Ξ of $\sim 2.5 \times 10^{11}$ W/cm².

Therefore, this calculation predicts that quantum interference can be used to inject ballistic currents in the plane of a quantum well with a characteristic velocity similar to that in bulk semiconductors.^{3,4} Although the proof-of-principle demonstration of carrier motion reported in this paper does not directly measure carrier velocity, it does provide evidence that the quantum interference control effect that was previously used to inject ballistic charge currents in bulk semiconductors^{2–4} can also be used to inject currents into quantum wells.

Finally, note that the dynamics of transport can be quite complex, involving more than just the injection rate of electrons and their characteristic velocities. Specifically, the schematic in Fig. 2(a) is overly simplistic, as it only shows electron motion. What is not shown is that holes move in the opposite direction to electrons, but with lower ballistic velocities due to their larger effective masses. Momentum relaxation will slow both electrons and holes (probably at different rates), and the space-charge field resulting from the separation of electrons and holes should pull both electron and hole distributions back toward $r=0$.¹⁰ However, the data in Figs. 4 and 5 demonstrate that the initial ballistic motion, combined with relaxation and space-charge field effects, results in a net shift of carrier density away from $r=0$ for our experimental conditions.

A thorough analysis of the carrier motion resulting from the complex interplay of injection, relaxation and space-charge effects is beyond the scope of this article. In future studies, optically probing carrier motion using techniques similar to those described in this paper could allow the study of these complicated transport dynamics, which have not been accessible when monitoring these currents with electrodes.

VI. SUMMARY

We have demonstrated that quantum interference between two- and one-photon absorption of ω and 2ω pulses with parallel linear polarizations produces a ballistic net charge current in GaAs/AlGaAs quantum wells. By controlling the phase difference between ω and 2ω , we can control the magnitude and sign of the current. This QUIC charge current was previously studied using electrodes in bulk material, but in this article we report an optical measurement of the carrier motion resulting from this current, and we provide the first demonstration of this QUIC net charge current in quantum wells. In future studies, this may facilitate direct study of the effects of confinement and/or strain on ballistic electron transport in semiconductor heterostructures.

ACKNOWLEDGMENTS

The authors thank Eric Gansen, Scot Hawkins, and Oleg Prepelita for insightful conversations. This work was supported in part by the Office of Naval Research, the Defense Advanced Research Projects Agency, Photonics Research Ontario, and the Natural Science and Engineering Research Council of Canada. A.N. acknowledges support from an Ontario Graduate Scholarship and the Walter C. Sumner Foundation.

¹E. Dupont, P. B. Corkum, H. C. Liu, M. Buchanan, and Z. R. Wasilewski, *Phys. Rev. Lett.* **74**, 3596 (1995).

- ²A. Haché, Y. Kostoulas, R. Atanasov, J. L. P. Hughes, J. E. Sipe, and H. M. van Driel, *Phys. Rev. Lett.* **78**, 306 (1997).
- ³A. Haché, J. E. Sipe, and H. M. van Driel, *IEEE J. Quantum Electron.* **34**, 1144 (1998).
- ⁴H. M. van Driel and J. E. Sipe, in *Ultrafast Phenomena in Semiconductors*, edited by K.-T. Tsen (Springer, New York, 2001), pp. 261–307, and references therein.
- ⁵J. M. Fraser, A. Haché, A. I. Shkrebtii, J. E. Sipe, and H. M. van Driel, *Appl. Phys. Lett.* **74**, 2014 (1999).
- ⁶N. Laman, A. I. Shkrebtii, J. E. Sipe, and H. M. van Driel, *Appl. Phys. Lett.* **75**, 2581 (1999).
- ⁷M. J. Stevens, A. L. Smirl, R. D. R. Bhat, J. E. Sipe, and H. M. van Driel, *J. Appl. Phys.* **91**, 4382 (2002).
- ⁸M. J. Stevens, A. L. Smirl, R. D. R. Bhat, A. Najmaie, J. E. Sipe, and H. M. van Driel, *Phys. Rev. Lett.* **90**, 136603 (2003).
- ⁹J. Hübner, W. W. Rühle, M. Klude, D. Hommel, R. D. R. Bhat, J. E. Sipe, and H. M. van Driel, *Phys. Rev. Lett.* **90**, 216601 (2003).
- ¹⁰D. Côté, J. M. Fraser, M. DeCamp, P. H. Bucksbaum, and H. M. van Driel, *Appl. Phys. Lett.* **75**, 3959 (1999); D. Côté, N. Laman, A. Springthorpe, and H. M. van Driel, (unpublished).
- ¹¹R. D. R. Bhat and J. E. Sipe, *Phys. Rev. Lett.* **85**, 5432 (2000).
- ¹²A. Najmaie, R. D. R. Bhat, and J. E. Sipe, *Phys. Rev. B* (to be published).
- ¹³J. M. Fraser, A. I. Shkrebtii, J. E. Sipe, and H. M. van Driel, *Phys. Rev. Lett.* **83**, 4192 (1999).
- ¹⁴M. J. Stevens, R. D. R. Bhat, J. E. Sipe, H. M. van Driel, and A. L. Smirl, *Phys. Status Solidi B* **238**, 568 (2003).
- ¹⁵While the relative phases of $\Delta T(\Delta\phi)$ at different probe positions can be inferred from the data in Fig. 4, the absolute phase was not determined.
- ¹⁶S. D. Ganichev, E. L. Ivchenko, S. N. Danilov, J. Erms, W. Wegscheider, D. Weiss, and W. Prettl, *Phys. Rev. Lett.* **86**, 4358 (2001).
- ¹⁷S. D. Ganichev, E. L. Ivchenko, V. V. Bel'kov, S. A. Tarasenko, M. Sollinger, D. Weiss, W. Wegscheider, and W. Prettl, *Nature (London)* **417**, 153 (2002).
- ¹⁸J. E. Sipe and A. I. Shkrebtii, *Phys. Rev. B* **61**, 5337 (2000).